

## COMPARISON OF MEASURED VS. MODELED $TE$ AND $TM$ FIELD PENETRATION INTO A SLOTTED CIRCULAR CYLINDER

**M. L. Waller and T. H. Shumpert**

Redstone Test Center (Provisional)  
TEDT-RT-ECE, E3 Test Division, Redstone Arsenal, AL 35898, USA

**R. W. Scharstein**

Electrical Engineering Department  
University of Alabama  
101 Houser Hall, Tuscaloosa, AL 35487-0286, USA

**S. H. Wong**

AFRL/RCM (High Performance Technologies, Inc.)  
2435 Fifth Street, Bldg. 676  
Wright-Patterson AFB, OH 45433-7802, USA

**Abstract**—In implementing electromagnetic vulnerability (EMV) testing on operational helicopters fielding a variety of avionic, communication, and weapons systems, the testing levels as spelled out in MIL-STD-464A require most test labs to position the high power source antennas unreasonably close to the test item (sometimes within 2 m). Questions naturally arise concerning the efficacy of such testing with respect to both the manner of coupling of the fields to the helicopter systems as well as the levels required to achieve reasonable confidence in the coupling effects. This paper presents a comparison of the electric fields interior to an axially slotted circular cylinder and the fields in the slot aperture as a function of the distance from the source to the test item. Also, these measured interior and aperture fields are compared to two different mathematical/numerical models of the conducting cylinder with an axial slot running the length of the cylinder. Additional measurements are presented for the fields interior to a finite cylinder with conducting endcaps and a significantly reduced slot of finite length. Comparisons to one of the mathematical/numerical models for this finite length cylinder with finite length slot are presented also.

---

*Received 30 November 2010, Accepted 9 February 2011, Scheduled 11 February 2011*  
Corresponding author: Marsellas L. Waller (marsellas.waller@gmail.com).

## 1. INTRODUCTION

In the testing of military systems and subsystems for electromagnetic vulnerability (EMV) and hazards of electromagnetic radiation to ordnance (HERO), extremely high amplitude (peak and rms) electromagnetic fields must be generated and radiated to immerse the system/subsystem in the required electromagnetic field environment [1, 2].

For some frequencies, the rms (and peak) electric field values can be hundreds (and thousands) of volts per meter, respectively. These inordinately high field levels often force test engineers to compromise in their approach in providing the required field environment levels. These high field levels are specified as uniform plane-wave fields that totally immerse the vehicle (such as would be radiated from remote high power communication and/or radar antennas). However, these system/subsystem level tests on vehicles such as rocket launchers, light armored vehicles, helicopters, etc. are frequently performed with a broadband radiating test antenna placed extremely near the test item to achieve these high electromagnetic levels (sometimes within 2 m). In light of this compromise, a natural question arises on the efficacy of such tests and the interpretation with respect to the vulnerability/safety of the systems/subsystems under test. As a required part of testing these systems to high intensity fields, often personnel are required to be positioned interior to the vehicles during the test. As a safety requirement, the interior fields at the positions where personnel are located must be measured prior to system level testing, and for field amplitudes exceeding the recommended levels for human exposure, the subsequent radiating power must be reduced and/or the time the personnel are exposed to these excessive field levels must be limited. In a previous analysis [3], a solution was presented for the interior fields and the fields in the aperture of an infinite slotted cylinder for the hard or  $TE$  polarization. Additional modeling has provided an accompanying model for the  $TM$  polarization excitation of the infinite slotted cylinder.

## 2. DESCRIPTION OF PHYSICAL CYLINDER AND FIELD MEASUREMENTS

Subsequent to these efforts modeling the coupling to an infinite slotted cylinder, a physical structure has been assembled and efforts have been carried out measuring the fields coupled into the slotted cylinder from antennas located at three separate distances away from the conducting cylinder. Specifically, an aluminum cylinder was constructed of five individual sections, each 1.219 m (4 ft) in diameter and 1.524 m (5 ft) in

length, with axial slots of approximately 0.2128 m (8 3/8 in) in width and 1.524 m (5 ft) in length. This slot width is consistent with an aperture angle of 20 degrees as measured from the two aperture edges to the center of the hollow cylinder. These five slotted sections are “mated” end-to-end to produce a hollow aluminum cylinder of 1.219 m in diameter and of 7.62 m (25 ft) in total length with a continuous slot running the total length of the cylinder with an opening of 20 degrees. (Internal physical support for maintaining the circular cross section of this hollow cylinder consists of non-conducting (dielectric) circular rings interior to these aluminum sections. A circular support is placed at each junction between the 5 ft sections. One circular dielectric plate is located at the center of the “center” section to allow for mounting and positioning the electric field probe.) This 25 ft cylinder is placed in a large anechoic chamber (with floor treatment) and positioned near one end broadside to the source antennas located at several distances away from the cylinder at the other end of the anechoic chamber. The “open ends” of this slotted cylinder are approximately 0.5 m from the “side” walls of the anechoic chamber (thus absorbing energy that might propagate down the length of this cylindrical “waveguide”). It is hoped that this arrangement of the cylinder and anechoic walls might approximate, physically and electromagnetically, an infinite cylinder with an infinite axial slot aperture. Fig. 1 shows the fabricated conducting slotted cylinder and one of the source antennas. (The forward tip of the log periodic dipole array (LPDA) in this configuration is 1 m from the slot). The surrounding anechoic chamber can be seen in the background.)

Measurements were made of the amplitudes of the electric fields (all three orthogonal components) in the interior of the cylinder and in the slot aperture in the center plane of the cylinder. (See Fig. 2 for a sketch of the cylinder cross section with one probe position in the center of the slot and with 13 specific positions interior to the cylinder.) Measurements were made with three different types of source antennas (biconical dipole, LPDA, and ridged horn antenna). For the initial measurements, each of these antennas was positioned as far away from the cylinder as convenience would allow. (The biconical dipole and the ridged horn were positioned at 7 m while the LPDA was positioned at 5 m.) Electric field amplitudes were measured with a Lindgren HI 6005 electric field probe driving a Lindgren FM 5004 field monitor with accompanying fiber-optic link. This probe was calibrated through appropriate commercial standards prior to its use in this measurement study. This probe has three diode-loaded dipoles oriented orthogonally to provide the three orthogonal components of the measured electric field. The monitor “reads” these three independent field components

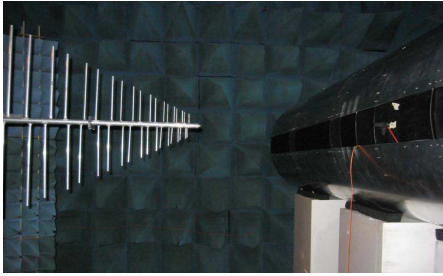


**Figure 1.** Measurement test setup on a 25 ft slotted circular cylinder.

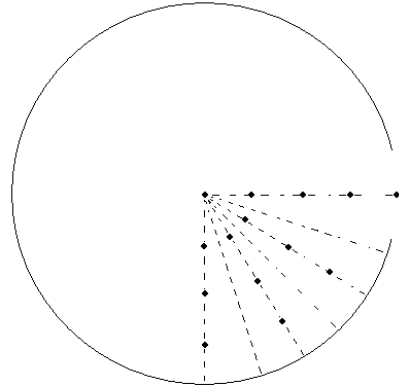


**Figure 2.** Cylinder cross section with internal and aperture probe positions.

as well as combining these three amplitudes into a total field amplitude that will be referred to in these measurements as the composite field. The gross physical dimension of this electric field probe is approximately  $3 \frac{3}{8}$  inches (approximately  $1/12$  of a wavelength at 100 MHz, and  $1/3$  of a wavelength at 400 MHz, respectively).

### 3. MEASURED AND MODELED ELECTRIC FIELDS FOR CYLINDER

Figures 3 and 4 give a comparison of the measured field amplitudes (composite amplitude of the three orthogonal components) for both *TE* and *TM* polarization in the aperture of the slot as produced by the three distinct antennas radiating a common applied free field of 20 V/m at the position of the open slot aperture when the cylinder is NOT present. *TE* polarization is defined to be the orientation of the source antenna when the electric field polarization is transverse to the longitudinal axis of the cylinder. For our physical case this means that the (dominant) electric field of the source antenna was vertical. *TM* polarization is defined to be the orientation of the source antenna when the electric field polarization is parallel to the longitudinal axis of the cylinder. For our physical case this means that the (dominant) electric field of the source antenna is horizontal. (Note: The acceptable frequency range of the biconical dipole was 100 MHz to 300 MHz; the range of the ridged horn was 180 MHz to 400 MHz, and the range of the LPDA was 100 MHz to 400 MHz.) Additional measurements (not

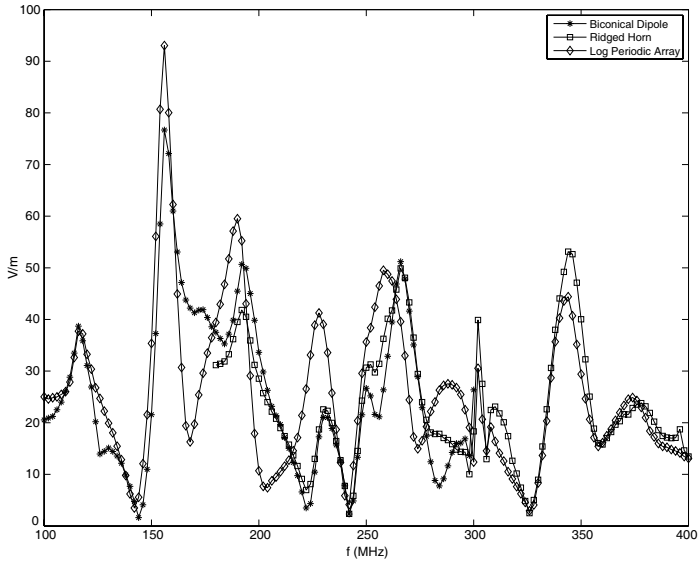


Figure 3. Measured aperture fields, vertical/ $TE$ .

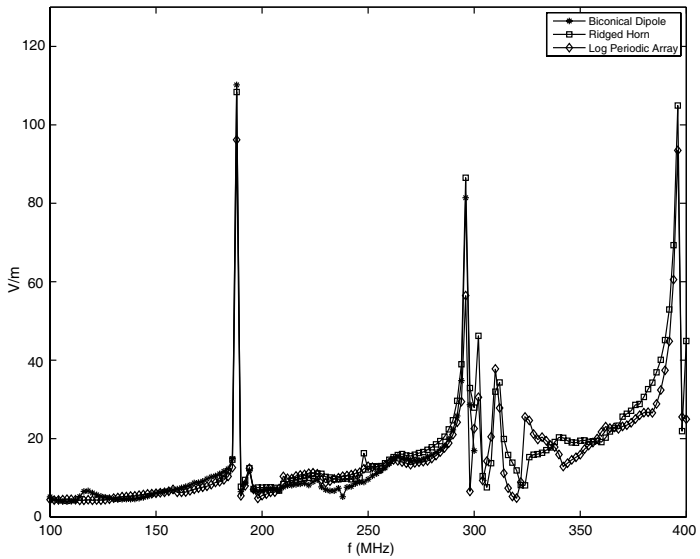


Figure 4. Measured aperture fields, horizontal/ $TM$ .

included here) were made of the electric fields at two interior points (one point on the cylinder axis and one point halfway between the axis and the aperture). These interior fields compared extremely well for the three different source antennas indicating the nature of the dominance of the interior fields on the cylinder structure rather than on the specific source antenna type.

The result of comparing the fields in the slot aperture measured from these three distinct sources was encouraging. These measurements confirmed experimentally that as long as the distance from the source is at least several wavelengths, the incident field environment is essentially a plane wave with little dependence on the actual geometry or type of radiating antenna. The enhanced values of the fields in Fig. 3 produced by the LPDA at  $\sim 190$  MHz and at  $\sim 230$  MHz as compared to those produced by the other two antenna types suggest some lack of polarization “purity” for the fields radiated by the LPDA. There was initial concern as to the effect of this cross-polarization radiation from the LPDA. Additional measurements confirm that the cross-polarization components of the LPDA are acceptably lower ( $< 13$  dB) than the dominant component. Subsequent to these measurements with each of the three distinct antennas acting as the source, it was decided to carry out all additional measurements with the LPDA as the primary source antenna (because it covers the entire frequency range of interest).

A variety of measurements of the fields in the aperture of the slot (always measured on the symmetry plane at the center (end-to-end) of the cylinder) have been carried out over a frequency range of 100 MHz to 400 MHz in 2 MHz steps. For the initial set of measurements, the source LPDA is positioned (forward tip) 5 m from the slot aperture of the cylinder. (The cylinder and source antenna are positioned such that the illumination is broadside to the cylinder and the source antenna is supported at such a height as to “shine” directly into the slot aperture. Of course, inasmuch as the floor of the anechoic chamber is treated, the height of the source antenna should have no consequence on the measurements except for positioning of the “infinite” slot with respect to the source position. All measurements were made with the source “shining” directly into the slot.)

Figures 5 and 6 present the measured electric field amplitudes (composite of all three orthogonal components) in the center of the slot aperture for both  $TE$  and  $TM$  polarizations. Superimposed on these measured values are predictions using an infinite series solution for the fields in the infinite axial slot in the two-dimensional infinite length cylinder (dashed curve). The coupling into the infinitely long cylinder (a two-dimensional problem) is evaluated by constructing

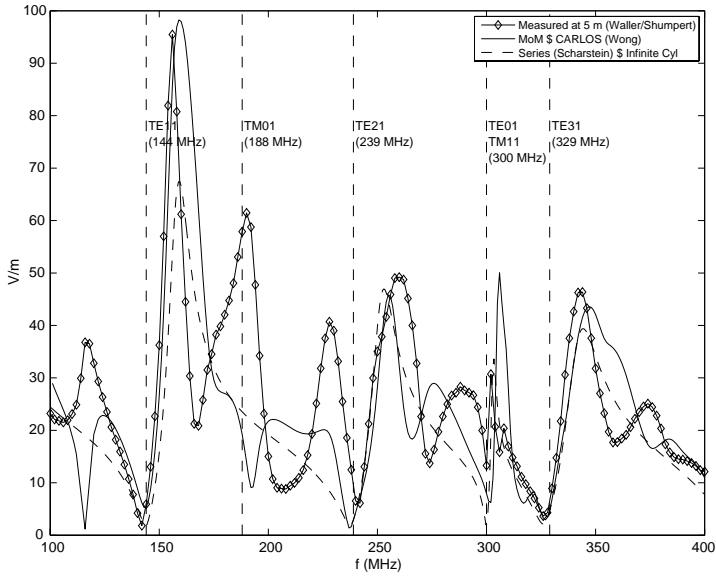


Figure 5. Aperture fields, vertical/ $TE$ .

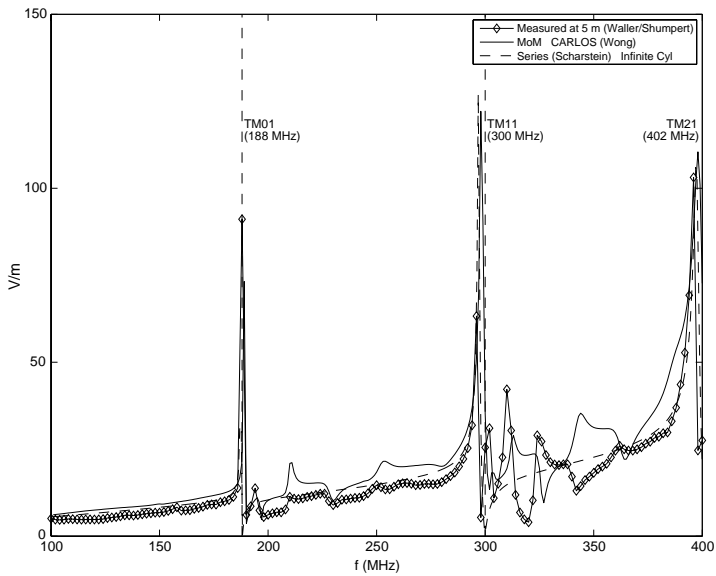


Figure 6. Aperture fields, horizontal/ $TM$ .

and solving Fredholm integral equations for the aperture fields. In the case of the  $TE$  or hard polarization, Green functions for the interior and exterior of the cylinder are used, resulting in a single-layer potential representation for the aperture field. Contrarily, direct eigenfunction expansions for the various fields themselves are used for the case of  $TM$  or soft polarization. In both cases, appropriate edge-condition weighted Chebyshev polynomials are used in a Galerkin formulation that explicitly includes the expected static behavior in the aperture geometry. Series acceleration techniques that also exploit the dominant, asymptotic physics by extracting the singular nature of the static contributions results in nicely convergent and demonstrably accurate numerics. Also, predictions using a three-dimensional moment method code (CARLOS) [4] for the finite Perfect Electric Conductor (PEC) cylinder with an axial slot running the length of the cylinder (solid curve) with incident plane wave excitation are presented. A number of observations concerning these plots are in order. First, it is encouraging for both modeling and measurements to see the correlation between results obtained on a two-dimensional model that specifically addresses the infinite slotted cylinder (series solution), a three-dimensional model of the 25 foot long finite cylinder with axial slot (moment method), and measurements made on the actual “physical” finite length slotted cylinder in the anechoic chamber. Prior to these measurements, it was hoped (and assumed) that one would “see” evidence in the slot aperture fields of the expected internal resonances associated with the circular cylinder  $TE$  and  $TM$  modes. Indeed, these modes are clearly present in both the measured and modeled aperture fields. Previous researchers (modelers) have predicted similar coupling to the infinite slotted cylinder [5, 6] including “upshifts” for the frequencies associated with the infinite slotted cylinder for  $TE$  polarization (Fig. 5) and slight “downshifts” for the  $TM$  polarization (Fig. 6). What is most surprising about the comparisons of the measured and modeled data is the excellent correlation between the amplitudes of the measured aperture fields and the modeled aperture fields. (The amplitudes of the aperture fields for each of the mathematical models and for the measured values have not been normalized in any manner other than the direct attempt to excite the respective slotted cylinder with a plane wave incidence with a free “calibrated” electric field of 20 V/m.) Prior to carrying out these measurements, it was decided to sample in frequency in 2 MHz steps. Unfortunately, careful perusal of the measured data (and comparisons with the modeled fields) suggests this sampling in frequency may have been too coarse to “see” all of the actual behavior in frequency of the amplitudes of these interior cylinder mode resonances.

As expected, the cylindrical modes for the  $TE$  cases are, in ascending order, TE11-144 MHz, TE21-239 MHz, TE01-300 MHz, and TE31-329 MHz). Hollow, closed cylinder modes are labeled and indicated with vertical dashed lines in Fig. 5. Two additional modes are clearly present in the  $TE$  data that appear to be concomitant  $TM$  modes (TM01-188 MHz) and TM11-300 MHz) that are probably being excited by the cross-polarized component radiated by the LPDA antenna. Several other measured responses are also noticeable in the data of Fig. 5. These appear at 116 MHz, 228 MHz, 288 MHz, and 373 MHz. These four responses do not appear in the two dimensional mathematical model. They may indeed be evidence that the actual experimental cylinder (finite length with physical asymmetries including the presence of the non-symmetrical electric field probe) does not actually lend itself mathematically to being separable into  $TE$  and  $TM$  mode superpositions. These modes may be referred to as hybrid modes that cannot be attributed to either  $TE$  or  $TM$  spatial decompositions. Scrutinizing the curves in Fig. 6 leads one to similar analysis. The expected cylindrical modes for the  $TM$  cases are, in ascending order, TM01-188 MHz, TM11-300 MHz, and TM21-402 MHz. As was done in Fig. 5, the hollow, closed cylinder modes are labeled and indicated with vertical dashed lines in Fig. 6. Again, other responses appear at frequencies not associated with these expected  $TM$  cylindrical modes. These additional responses may be attributable to the “finiteness” of the finite cylinder and any inherent asymmetries present in the physical case. Other researchers (modelers) have also observed the higher  $Q$ 's of the  $TM$  modes as compared to the  $Q$ 's of the  $TE$  modes. In addition, there seems to be much less excitation of the cross-polarized modes. This result may be a consequence of the fact that the  $TM$  excitation that couples through the slotted aperture experiences a waveguide cutoff (705 MHz) significantly above the location of these lower order  $TE$  and  $TM$  modes in this slotted cylinder. (Incidentally, because the slot is open for its entire length there is technically no lower cutoff frequency for the  $TE$  propagation through the slot.)

Additional measurements are shown in Figs. 7 and 8 presenting values of the “spatially averaged” fields induced interior to the slotted cylinder for the two polarizations,  $TE$  and  $TM$ . These curves represent interior electric fields measured at the 13 specific locations (illustrated previously in Fig. 2) and spatially averaged. The spatial averaging is done in a manner consistent with considering the maximum permissible exposure (MPE) levels of the permissible power densities for human exposure. Specifically, the composite electric field amplitude at each of the 13 unique, interior positions is squared, summed, and the square

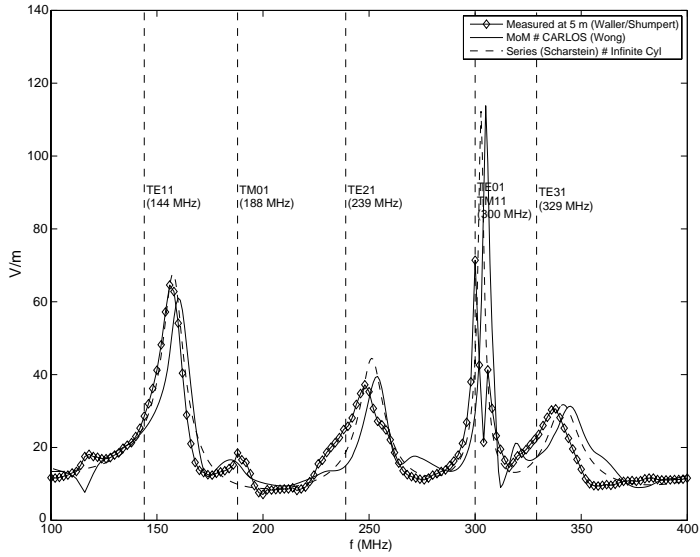


Figure 7. “Spatially averaged” internal fields, vertical/ $TE$ .

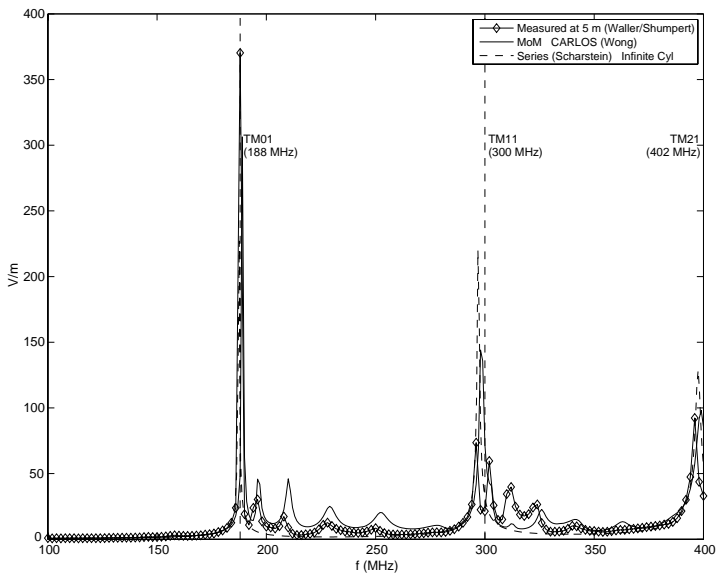


Figure 8. “Spatially averaged” internal fields, horizontal/ $TM$ .

root of this resulting sum represents the “spatially averaged” electric field in the interior of the cylinder. These interior fields also exhibit the same expected resonances in the  $TE$  and  $TM$  excitations. To be expected, the amplitudes of the measured “spatially averaged” interior fields compare extremely favorably with the “spatially averaged” values predicted by the two models. Such close amplitude agreement provides these researchers with significant confidence in the validity and procedures of their measured electric field values.

An additional observation can be made from the interior “spatially averaged” fields concerning the “shielding effectiveness” of this slotted cylinder, and the implications these data have for testing of vehicles when personnel are present in the interior “cavities” of the vehicle during high intensity field (EMV) testing. Note that Fig. 7 indicates an interior “spatially-averaged” electric field enhancement factor (relative to the applied free field of 20 V/m) of over 300% at  $\sim 155$  MHz, 190% at  $\sim 250$  MHz, and 350% at  $\sim 300$  MHz. Although it is apparent these significant enhancements occur at cavity resonances, it is also apparent that the “spatially-averaged” interior electric fields show some enhancement at many frequencies in this 100 MHz to 400 MHz range. The data for the  $TM$  case (Fig. 8) is even more pronounced with the measured field enhancement exceeding 1500% at the first cylinder resonance.

The following discussion of the significance of these “enhanced” field values on test procedures is useful. The 25 ft long, 4 ft diameter cylinder may be considered a highly idealized  $1/2$  scale model of the Blackhawk helicopter. Suppose one is carrying out EMV testing of a Blackhawk helicopter where one of the test frequencies is very near an interior “cockpit resonance” of 77.5 MHz ( $1/2$  of the 155 MHz,  $TE_{11}$  mode referenced above). Suppose the applied exterior free field is 200 V/m (ten times the 20 V/m applied in all of the field measurements included in this present study.) The rms field value permissible for human exposure for “controlled fields” by the current safety documents [7] is 61.4 V/m at a frequency of 77.5 MHz. Since the measured composite value scaled by the factor of ten) is approximately 600 V/m, the time allowed for the pilot (co-pilot) in this high “cockpit resonant” field would be a little less than 4 sec based on the allowable time constant of 6 minutes. Although it is highly unlikely that the actual cockpit resonant  $Q$  of a Blackhawk helicopter would be as high as the idealized cylinder  $Q$ , spatially-sampled and “averaged” internal fields measurements made inside an actual Blackhawk helicopter cockpit have significantly limited actual test time by an order of magnitude or more ( $< 36$  sec compared to the allowable 6 min).

As mentioned above, although the resonance “ $Q$ ’s” of this cylinder

greatly exceed the “Q’s” of realistic vehicle cavities, interior field measurements made inside real vehicles exhibit enhanced interior fields at specific frequencies associated with cavity resonances. Such behavior is regularly observed in the interior of helicopter cockpits and cargo spaces while measuring (and spatially averaging) the interior fields produced during EMV tests. Such measurements regularly limit the time that personnel can be exposed at certain test frequencies during actual EMV testing on helicopters and ground vehicles with personnel occupying various cavities (cockpit, cargo area, cab, targeting positions, etc.) in real vehicles.

#### 4. FIELD COMPARISONS VS RANGE OF ANTENNA FROM CYLINDER

As indicated in the Introduction, one of the issues being addressed in these measured data was a comparison of the electric fields (aperture and interior) coupled to the cylinder by antennas located at different distances from the cylinder. Electric fields produced in the slotted aperture at two different source distances (1 m and 5 m from the tip of the LPDA to the aperture, respectively) are given in Figs. 9 and 10 for the two distinct polarizations,  $TE$  and  $TM$  respectively. The induced electric fields when the LPDA is moved to within 1 m (dots) exhibit somewhat different behavior than the 5 m data (x’s). First, it is observed that the amplitudes of the induced aperture fields at 1 m source distance are reduced by as much as 25–30% as compared to 5 m source distance (and corresponding plane wave model presented in Fig. 4) for  $TE$  excitation and are reduced by as much as 50–75% as compared to the 5 m source distance (and corresponding plane wave model presented in Fig. 6) for  $TM$  excitation, respectively. In addition to these amplitude reductions, it appears that mode peaks are significantly shifted in frequency (especially for the  $TE$  polarization) indicating some additional “loading” of the aperture by the source as well as excitation of additional modes. Indeed the mode structure and interpretation of the coupled aperture fields seems much more complicated and difficult to understand. Of course, all of these observations are no doubt influenced greatly by the fact that the source is radiating into the aperture with the “near-field” radiation of the LPDA. (See Fig. 11 for practical application of these issues.)

The immediate implications with respect to the reduced amplitudes are to bring into question whether current testing (being carried out in an identical manner to that demonstrated by this current measurement exercise) is sufficient to excite with adequate amplitude the various coupling mechanisms to electronic systems/subsystems

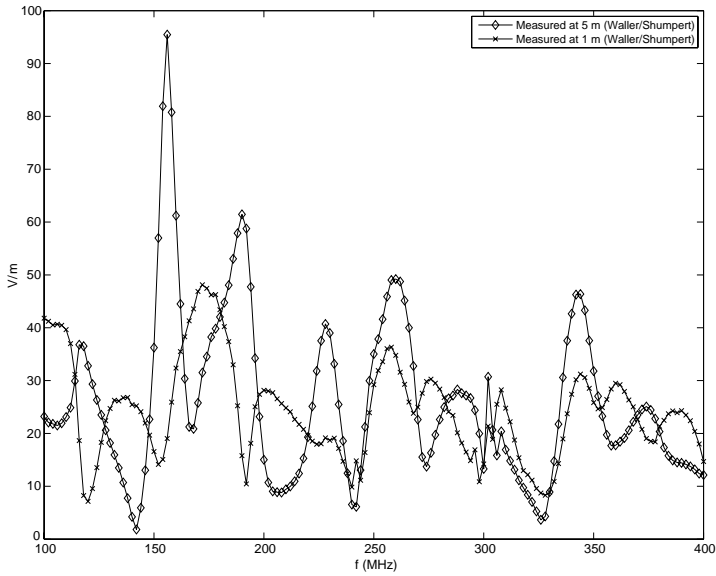


Figure 9. Measured aperture fields, vertical/ $TE$ .

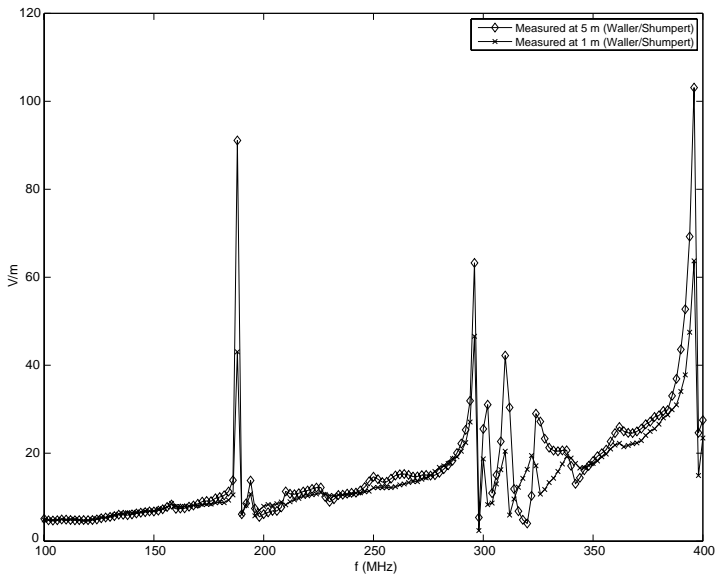


Figure 10. Measured aperture fields, horizontal/ $TM$ .



**Figure 11.** Typical EMV test setup.

interior to vehicles such as helicopters, ground command and control vehicles, rocket launchers, personnel carriers, etc. These current data are not encouraging that the practice of exciting these vehicles with source antennas located in such close proximity to the vehicle is recommended in future EMV testing. Further studies on more realistic structures are needed to address in a quantitative manner just how significant these differences are for real vehicles and their concomitant interior electronic sensitivities, as well as the implications for testing with high intensity fields when personnel are present inside the vehicles.

## 5. FINITE LENGTH CYLINDER WITH REDUCED-LENGTH FINITE SLOT

As a final example of the field interior to the cylinder, the physical cylinder was modified with conducting plates (disks) placed over the ends of the 25 foot cylinder, and the slotted aperture was “shorted” except for a 5 foot section in the center as seen in Fig. 12. Figs. 13 and 14 present the “spatially averaged” interior fields for both the  $TE$  and  $TM$  excitations with the LPDA positioned at a distance of 5 m and also at the much closer distance of 1 m. Superimposed upon these physical measurements is the coupling into the interior of the finite closed cylinder with reduced aperture from a plane wave produced by the moment method code (Wong-CARLOS).

As expected, shorting the ends of the 25 foot cylinder produces a significant number of additional interior “resonances” or modes associated with longitudinal variations in the closed conducting cylinder. It is apparent in these data that the longitudinally symmetric modes are present at frequencies closely associated with the interior resonances of the completely closed conducting cylinder (see Table 1).



**Figure 12.** Measurement test setup on a 25 ft “shorted” slotted circular cylinder.

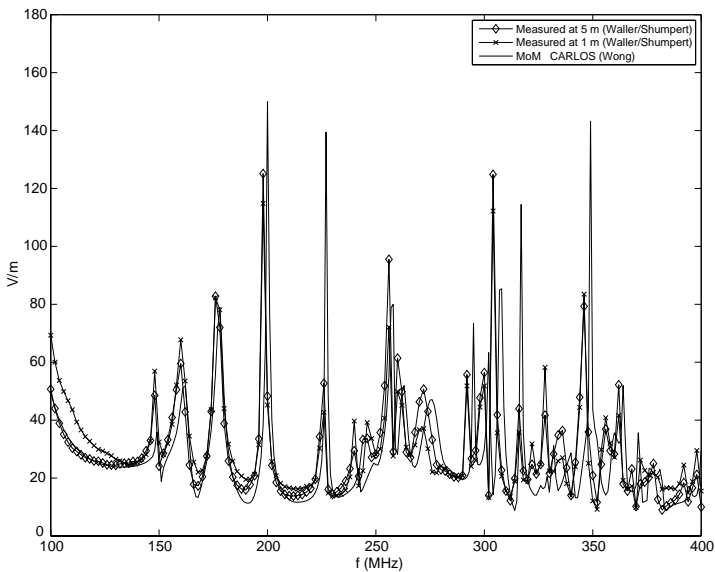


**Figure 13.** “Spatially averaged” internal fields, vertical/ $TE$ , “shorted cylinder.”

Again, in addition to the close frequency agreement of the measured “spatially averaged” interior fields with the modeled “spatially averaged” interior fields, it is interesting that the amplitude of the model interior fields are again quite comparable to those measured. These comparisons in both frequency and amplitude are again encouraging for both the validity of the measurements as well as the veracity and fidelity of the numerical model. It is also observed that the interior fields induced by the plane wave (model) and the

**Table 1.** TE and *TM* mode resonances (< 400 MHz) for the empty, closed conducting cylinder, 25 feet long and 4 feet in diameter.

q	TM11q TE01q	TE11q	TE21q	TE31q
1	300.553	145.446	239.863	329.415
3	305.659	155.725	246.232	334.081
5	315.625	174.476	258.500	343.222
7	330.010	199.321	275.878	356.495
9	348.266	228.280	297.476	373.637
11	369.821	259.981	322.444	393.637
13	394.134	293.538	350.064	
15		328.382	379.756	
17		364.143		

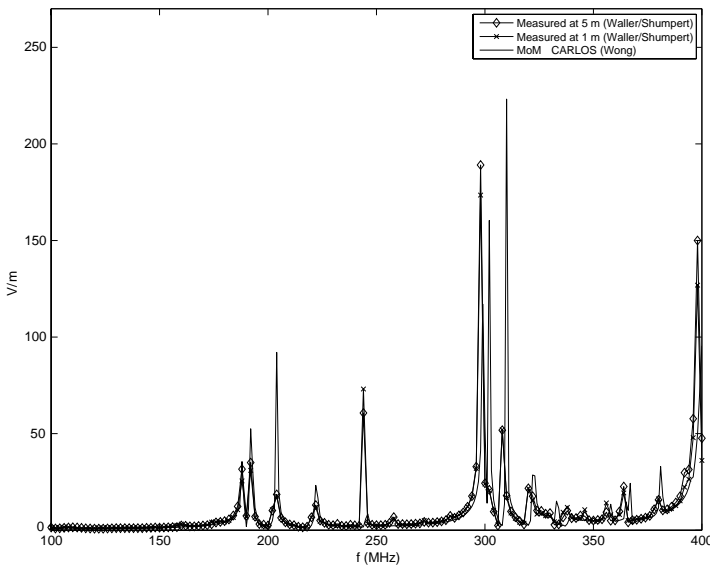


**Figure 14.** “Spatially averaged” internal fields, horizontal/*TM*, “shorted cylinder.”

physical antenna located 5 m away from the cylinder are more similar in frequency and spatial variations to that produced by the physical source antenna located on 1 m away from the cylinder. This “closer” agreement between the 5 m source and the 1 m source may be due to the fact that the near fields of the source LPDA at 1 m do not

“couple” into the finite aperture as “easily” as for the infinite slotted aperture case. For the most part, the  $Q$ 's of the predicted (modeled) field interior to the cylinder are considerably higher than those of the physically measured fields.

Again, it is noticed that the number of  $TE$  modes greatly exceeds the number of  $TM$  modes for this closed-end slotted cavity. This may again be a consequence of the “cutoff” frequencies of the aperture. The cutoff for propagation of the  $TE$  polarized energy through the finite aperture is approximately 98 MHz whereas the cutoff frequency for the propagation of the  $TM$  polarized energy through the finite aperture is approximately 705 MHz. Obviously, the  $TM$  modes inside the cavity must be excited by evanescent fields traversing the slot aperture.

## 6. CONCLUSION

A physically large conducting (aluminum) cylinder was constructed with a longitudinal slot running its entire length. This slot represents an opening into the cylinder of approximately 20 degrees relative to its complete circumference. Electric fields were measured in the slot aperture and at several locations inside the cylinder in a plane along the center line with respect to a radiating source antenna (LPDA) located at some distance from the cylinder radiating “broadside” to the cylinder and “shining” directly into the open slotted aperture. These measured aperture and interior fields were compared to two different mathematical/numerical models that calculated the fields coupled onto the slotted aperture and into the interior of the cylinder. These comparisons of measured and modeled fields exhibited many similarities in both their behavior with respect to frequency as well as close correlations between the measured and calculated electric field amplitudes. Instances where the measured and modeled fields were significantly different were pointed out, and possible explanations for these differences were proffered. Comparisons were made between aperture and interior fields for source antennas located at two different distances representing approximate far-field plane wave excitation and near-field non-planar excitation by the same antenna. Differences between these two cases are also addressed and observations as to some of the possible reasons and implications for testing are tendered. Finally, measured and modeled “spatially-averaged” electric fields interior to a closed-ended finite cylinder with a reduced finite length slot are presented. These results are compared and discussed.

## ACKNOWLEDGMENT

Special appreciation is given to Leonel E. Najera, the ERC Inc. lead technician for measurements on this project, for his attention to detail and hard work ethic.

The authors would like to thank the DoD High Performance Computing Modernization Program for providing the computational resources for the moment method simulations performed in this work.

## REFERENCES

1. *Electromagnetic Environmental Effects Requirements for Systems*, Department of Defense Standard, MIL-STD-464A, December 19, 2002.
2. *Electromagnetic Environmental Effects (E3) Performance and Verification Requirements*, Aeronautical Design Standard, ADS-37A-PRF, May 28, 1996.
3. Scharstein, R. W., M. L. Waller, and T. H. Shumpert, "Near-field and plane-wave electromagnetic coupling into a slotted circular cylinder: Hard or  $TE$  polarization," *IEEE Trans. on Electromag. Comp.*, Vol. 48, No. 4, 714–724, Nov. 2006.
4. Putnam, J. M. and M. B. Gedera, "CARLOS-3D: A general-purpose three-dimensional method-of-moments scattering code," *IEEE Antennas & Propagation Magazine*, Apr. 1993.
5. Beren, J. A., "Diffraction of an  $H$ -polarized electromagnetic wave by a circular cylinder with an infinite axial slot," *IEEE Trans. on Ant. and Prop.*, Vol. 31, No. 30, 419–425, May 1983.
6. Ziolkowski, R. W. and J. B. Grant, "Scattering from cavity-backed apertures: The generalized dual series solution of the concentrically loaded  $E$ -pol slit cylinder problem," *IEEE Trans. on Ant. and Prop.*, Vol. 35, No. 5, 504–528, May 1987.
7. *Protecting Personnel from Electromagnetic Fields*, Department of Defense Instruction, DODi 6055.11, August 19, 2009.